Available online at www.sciencedirect.com
SCIENCE DIRECT®
Journal of Sound and Vibration 293 (2006) 1–15
JOURNAL OF SOUND AND VIBRATION
www.elsevier.com/locate/jsvi

Dynamic behavior of a coupled elastic shaft–elastic beam system

H. Diken*

Mechanical Engineering Department, King Abdulaziz University, P.O. Box 80204, Jeddah 21589, Saudi Arabia

Received 26 February 2004; received in revised form 20 May 2005; accepted 19 September 2005
Available online 7 November 2005

Abstract

In this study, a servomotor-driven coupled elastic shaft–elastic beam system is analyzed. The model consists of a servomotor, elastic shaft, disk, and an elastic beam attached to the disk. Equations of motion are derived with respect to the generalized coordinates of the elastic shaft and elastic beam. Nondimensional parametric equations are obtained. Three independent parameters are defined affecting the system. These are the rigidity factor, the ratio of the beam inertia to total inertia, and the ratio of the shaft inertia to total inertia. Simulations demonstrate the important role of these three parameters in the behavior of the system.

1. Introduction

Servomotors are rapidly replacing conventional ones. The introduction of servomotors has increased the importance of transient motion analysis, which is becoming increasingly important and critical in the design of automated machines. This is why position control of mechanical systems with structural flexibility has been an important research area in recent years.

El-Sinawi and Hamdan [1] developed a new approach based on the linear quadratic estimator technique for estimating the vibration of any point on the span of a rotating flexible beam mounted on a compliant hub in the presence of process and measurement noise. Nassar and Bedoor [2] developed a general model to describe the rotating blade vibration under the effect of shaft torsional vibration. Al-Bedoor et al. [3] has developed a mathematical model for a flexible arm undergoing large planar flexural deformation, continuously rotating under the effect of a hub torque and supported by a flexible base.

Diken [4] studied a model consisting of a servomotor, harmonic drive, flexible shaft and a manipulator arm, which can be considered as a rigid beam. The transfer function of the system, relating the desired input rotation to the manipulator arm rotation is developed. Natural frequency and damping ratio of the flexible system, together with PID control parameters, appear in the transfer function. The possibility of precise trajectory tracking is discussed. Diken [5] has also studied a similar dynamic model for the frequency response analysis. It is shown that the control system damping ratio has an important role in the behavior of the system. For the low values of the damping ratio, system natural frequency is effective, for the high values of the

*Tel.: +966 2 640 2000.
E-mail address: hdiken@yahoo.com.

0022-460X/$ - see front matter © 2005 Published by Elsevier Ltd.
doi:10.1016/j.jsv.2005.09.011

damping ratio, subsystem natural frequency becomes effective on the system behavior. In Ref. [6], Diken also studied similar dynamic model consisting of an elastic shaft. In this study, the effect of the flexible system natural frequency and the substructural natural frequency is extensively analyzed and the fourth-order transfer function of the system is approximated to the second-order one. Ankarali and Diken [7] modeled a rotating Euler–Bernoulli beam and studied the residual vibration spectrum. It is shown that the residual vibration can be eliminated at certain values of the frequency of the rise function. Diken [8] also modeled rotating Euler–Bernoulli beam, which is actuated by servomotor. He obtained transfer function of the elastodynamic control system relating the beam rotation and the beam tip vibration to the desired servomotor rotation. Shear force at the root of the beam is used as a feedback for the control system. Parametric analysis is done and the effect of the shear force feedback control strategy on the beam tip vibration is studied.

Kopmaz and Anderson [9] obtained coupled nonlinear equations of a motion in a very general fashion considering the influence of the rotor, shaft, hub, beam and the payload as well as geometric stiffness terms, which arise from both centripetal and Coriolis accelerations. The solution concentrates on the effect of the two parameters representing the mass and the stiffness ratios of the manipulator system on its driveline. Xi and Fenton [10] and Xi et al. [11] investigated the coupling effect of a flexible link and a flexible joint in a one-link rotating structure. Flexible shaft is represented by a torsional stiffness but not considered as a distributed mass. They defined two nondimensional parameters; the ratio of a bending stiffness of the link to the torsional

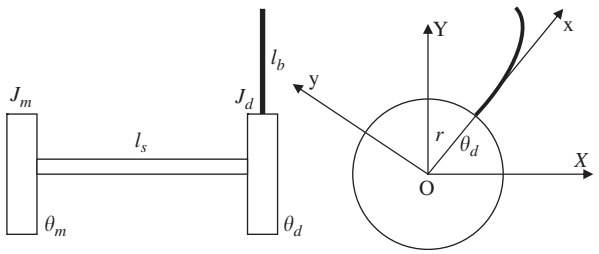

Fig. 1. Coupled elastic shaft and elastic beam system model.

Table 1
Values of β_s and $\phi_s(l_s)$

μ_s	β_s	$\phi_s(l_s)$
0.1	0.3111	0.3061
0.2	0.4328	0.4194
0.3	0.5218	0.4984
0.4	0.5932	0.5590
0.5	0.6533	0.6078

Table 2
First three values of $\beta_b l_b$

K	$(\beta_b l_b)_1$	$(\beta_b l_b)_2$	$(\beta_b l_b)_3$
0	1.8751	4.6941	7.8548
0.1	1.7227	4.3995	7.4511
1	1.2479	4.0311	7.1341
5	0.8700	3.9500	7.0825
25	0.5872	3.9314	7.0714
100	0.4159	3.9278	7.0693
1000	0.2340	3.9267	7.0687
∞	0	3.9266	7.0686

stiffness of the rotor–beam joint and the moment of inertia ratio of the link to the rotor. Separation of variables method is used to solve the dynamic equations. Frequency equation of the system is obtained and the effect of the defined parameters on the frequencies of the system is investigated.

In this study, a servomotor controlled elastic shaft, disk and an elastic beam, which is attached to the disk is modeled as an elastodynamic control system. Elastic shaft is considered as a distributed mass system, elastic beam is assumed as an Euler–Bernoulli beam. Because of the coupling, boundary conditions for the elastic beam changes from hinged-free beam to fixed-free beam depending on the stiffness of the elastic shaft. Nondimensional equations of the motion are obtained. Three parameters: the rigidity factor, the shaft inertia ratio, and the beam inertia ratio with respect to the total inertia are defined. The response of the elastic system to a step rotational input is simulated with respect to these parameters. The coupling effect of the free vibration of either shaft or beam on each other is also shown.

2. Formulation

Fig. 1 shows the elastic shaft–elastic beam model of the dynamic system.

The kinetic energy of the system can be written as

$$T = \frac{1}{2}J_m\dot{\theta}_m^2 + \frac{1}{2}J_d\dot{\theta}_d^2 + \frac{1}{2}\int_0^{l_b} m_b V_b^2 \,\mathrm{d}x + \frac{1}{2}\int_0^{l_s} \rho I_p \dot{\theta}_s^2 \,\mathrm{d}z. \tag{1}$$

Here J_m is the servomotor mass moment of inertia, $\dot{\theta}_m$ is the motor angular velocity, J_d is the disk inertia, $\dot{\theta}_d$ is the disk angular velocity, l_b is the beam length, m_b is the beam mass per unit length, V_b is the absolute velocity of m_b with respect to the fixed coordinate system OXYZ. l_s is the shaft length, ρ is the density of the shaft, I_p is

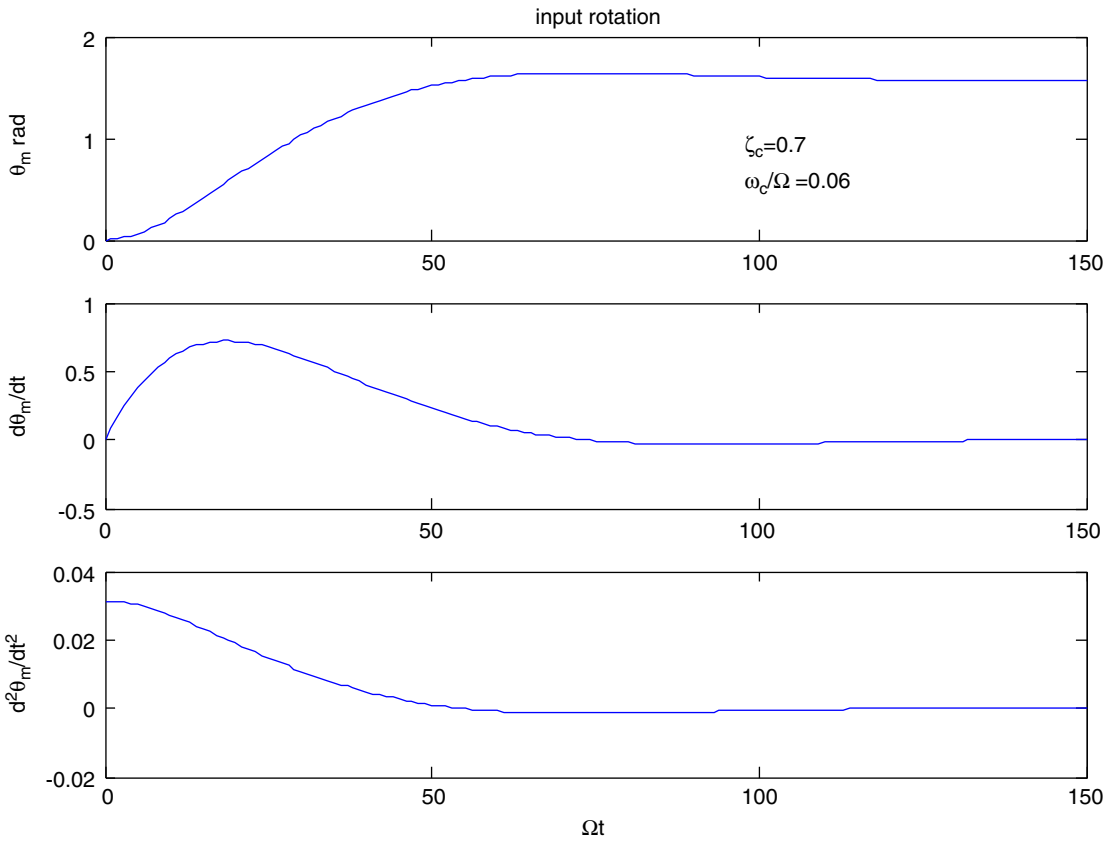

Fig. 2. Servomotor input rotation.

the polar area moment of inertia of the shaft, $\dot{\theta}_s$ is the shaft angular velocity. The potential energy of the system can also be given as follows:

$$U = \frac{1}{2}\int_0^{l_b} \mathrm{EI}y''^2(x,t)\,\mathrm{d}x + \frac{1}{2}\int_0^{l_s} \mathrm{GI}_p\psi'^2(z,t)\,\mathrm{d}z. \tag{2}$$

Here EI is the rigidity of the elastic beam, $y(x,t)$ is the deflection of m_b with respect to the rotating frame OXYZ, GI_p is the rigidity of the elastic shaft, $\psi(z,t)$ is the elastic rotation of the shaft. Virtual work because of the viscous damping of the elastic shaft and elastic beam can be given as

$$\delta W = -\int_0^{l_s} c_s\dot{\psi}(z,t)\,\mathrm{d}z\,\delta\psi - \int_0^{l_b} c_b\dot{y}(x,t)\,\mathrm{d}x\,\delta y. \tag{3}$$

Here c_s and c_b are viscous damping coefficients of the elastic shaft and elastic beam, respectively. Total shaft rotation is the sum of the servomotor rotation plus the elastic rotation of the shaft and disk rotation is the servomotor rotation plus the shaft rotation at the disk end.

$$\begin{aligned}\theta_s(t) &= \theta_m(t) + \psi(z,t),\\ \theta_d(t) &= \theta_m(t) + \psi(l_s,t).\end{aligned} \tag{4}$$

Square of the absolute velocity of the beam mass m_b with respect to the fixed frame OXYZ is obtained as

$$V_b^2 = (y\dot{\theta}_d)^2 + [(r+x)\dot{\theta}_d + \dot{y}]^2. \tag{5}$$

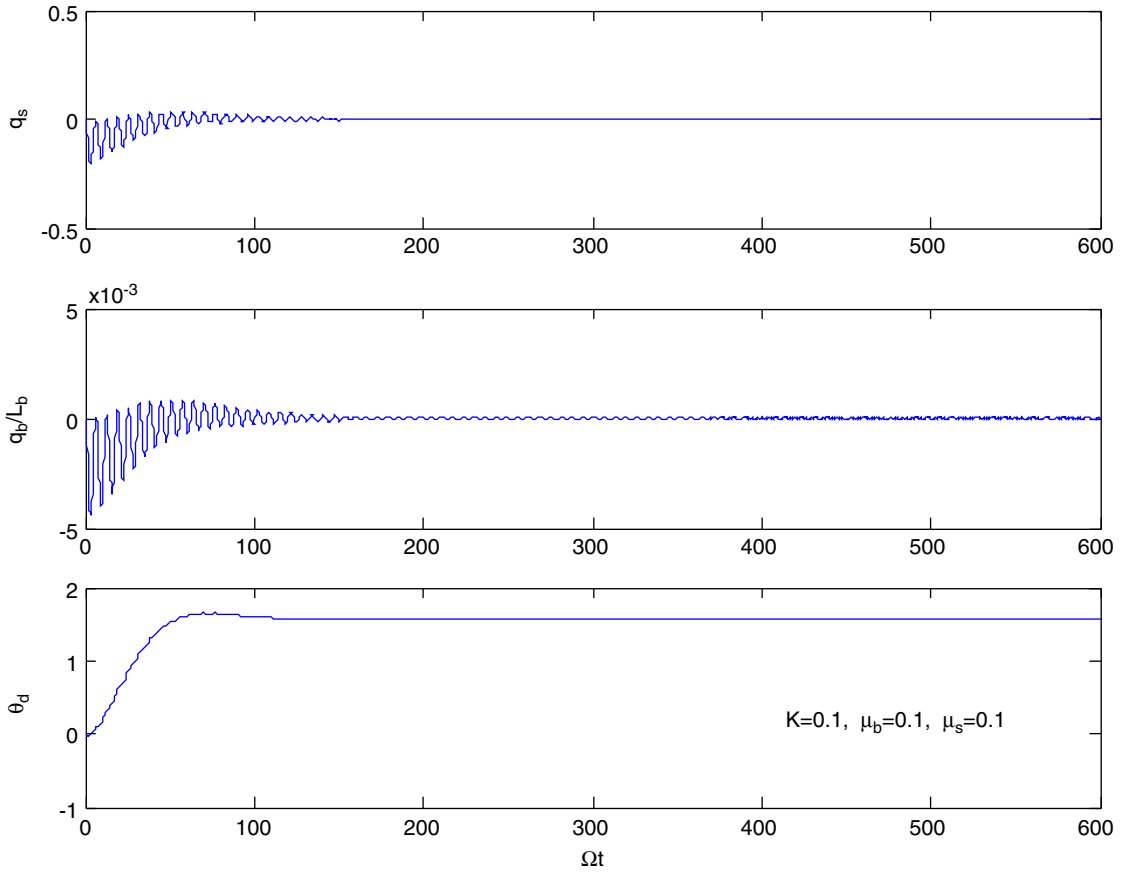

Fig. 3. Shaft, beam and disk response for $K = 0.1$, $\mu_b = 0.1$, $\mu_s = 0.1$.

Here r is the radius of the disk. Elastic shaft rotation and the elastic beam deflection are assumed as the sum of the orthogonal modes:

$$\begin{aligned}\psi(z,t) &= \sum \phi_s(z)q_s(t) \approx \phi_s(z)q_s(t),\\ y(x,t) &= \sum \phi_b(x)q_b(t) \approx \phi_b(x)q_b(t).\end{aligned} \tag{6}$$

In this study, only first modes are considered. When Eqs. (4), (5) and (6) are used, Eqs. (1), (2) and (3) will become

$$\begin{aligned}T = \frac{1}{2}J_m\dot{\theta}_m^2 + \frac{1}{2}J_d[\dot{\theta}_m + \phi_s(l_s)\dot{q}_s(t)]^2 + \frac{1}{2}\int_0^{l_b} m_b\{\phi_b(x)q_b(t)[\dot{\theta}_m + \phi_s(l_s)\dot{q}_s(t)]^2\\ + [(r+x)(\dot{\theta}_m + \phi_s(l_s)\dot{q}_s(t)) + \phi_b(x)\dot{q}_b(t)]^2\}\,\mathrm{d}x + \frac{1}{2}\int_0^{l_s}\rho I_p[\dot{\theta}_m + \phi_s(z)\dot{q}_s(t)]^2\,\mathrm{d}z.\end{aligned} \tag{7}$$

Potential energy is

$$U = \frac{1}{2}\int_0^{l_b} \mathrm{EI}\phi''^2_b(x)q_b^2(t)\,\mathrm{d}x + \frac{1}{2}\int_0^{l_s}\mathrm{GI}_p\phi'^2_s(z)q_s^2(t)\,\mathrm{d}z. \tag{8}$$

Virtual work is

$$\delta W = -\int_0^{l_s} c_s\phi_s^2(z)\dot{q}_s(t)\delta q_s(t)\,\mathrm{d}z - \int_0^{l_b} c_b\phi_b^2(x)\dot{q}_b(t)\delta q_b(t)\,\mathrm{d}x. \tag{9}$$

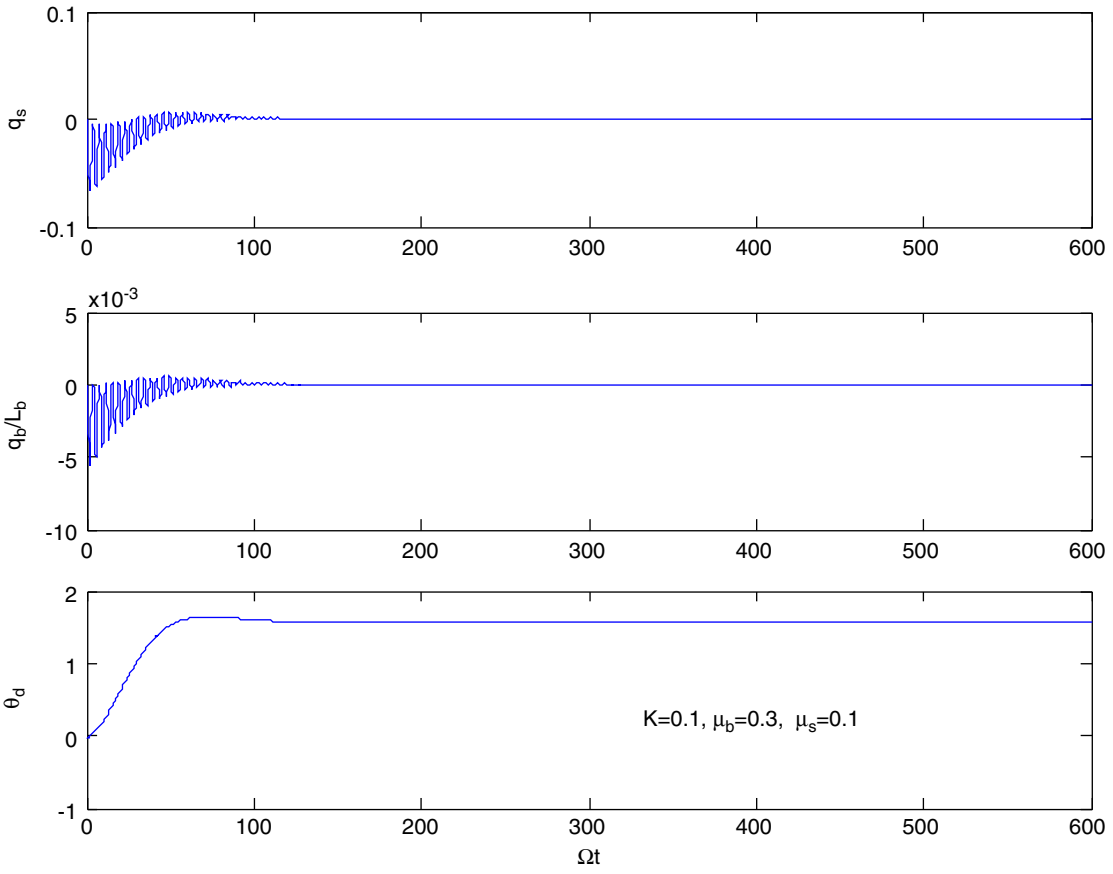

Fig. 4. Shaft, beam and disk response for $K = 0.1$, $\mu_b = 0.3$, $\mu_s = 0.1$.

Lagrange equations are used to obtain the governing equations of the system. Generalized coordinates are q_b and q_s. q_b and q_s are already small; higher-order terms will be smaller, that is why second- and third-order nonlinear terms like $q_b\dot{q}_b$, $q_b\dot{q}_b\dot{q}_s$, q_b^2, $q_b^2\ddot{q}_s$, $q_b\dot{q}_s^2$ are ignored and the following equations are obtained:

$$\begin{aligned} &\ddot{q}_s + 2\zeta_s\omega_t\dot{q}_s + \omega_t^2 q_s + m_{sb}\ddot{q}_b = -u_s\ddot{\theta}_m, \\ &\ddot{q}_b + 2\zeta_b\omega_b\dot{q}_b + \omega_b^2 q_b + m_{bs}\ddot{q}_s = -u_b\ddot{\theta}_m. \end{aligned} \tag{10}$$

Here torsional vibration damping ratio is

$$2\zeta_s\omega_t = \frac{c_s}{J_T}\frac{\int_0^1 \phi_s^2(\xi)\mathrm{d}\xi}{\phi_s^2(l_s)}, \frac{z}{l_s} = \xi. \tag{11}$$

Torsional vibration natural frequency is

$$\omega_t^2 = \frac{\mathrm{GI}_p}{l_s J_T}\frac{\int_0^1 \phi'^2_s(\xi)\,\mathrm{d}\xi}{\phi_s^2(l_s)}. \tag{12}$$

Mass coupling factor m_{sb} is

$$m_{sb} = \frac{m_b l_b^3}{J_T}\frac{\int_0^1((r/l_b)+\xi)\phi_b(\xi)\,\mathrm{d}\xi}{\phi_s(l_s)}. \tag{13}$$

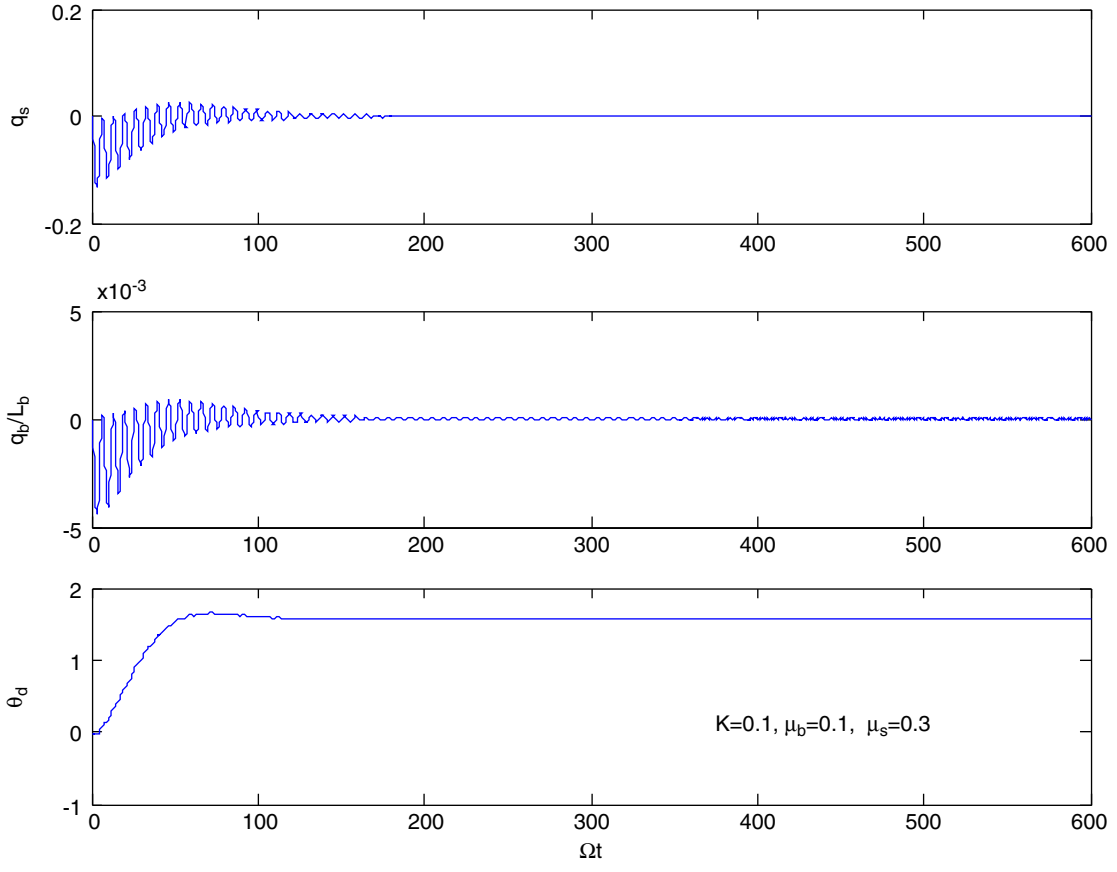

Fig. 5. Shaft, beam and disk response for $K = 0.1$, $\mu_b = 0.1$, $\mu_s = 0.3$.

Shaft mode participation factor is

$$u_s = \frac{1}{\phi_s(l_s)}. \tag{14}$$

Beam damping ratio is

$$2\zeta_b\omega_b = \frac{\int_0^1 c_b\phi_b^2(\xi)\,\mathrm{d}\xi}{\int_0^1 m_b\phi_b^2(\xi)\,\mathrm{d}\xi}, \frac{x}{l_b} = \xi. \tag{15}$$

Beam natural frequency is

$$\omega_b^2 = \frac{\mathrm{EI}}{m_b l_b^4}\frac{\int_0^1 \phi''^2_b(\xi)\,\mathrm{d}\xi}{\int_0^1 \phi_b^2(\xi)\,\mathrm{d}\xi}. \tag{16}$$

Mass coupling factor m_{bs} is

$$m_{bs} = \phi_s(l_s)\frac{\int_0^1((r/l_b)+\xi)\phi_b(\xi)\,\mathrm{d}\xi}{\int_0^1 \phi_b^2(\xi)\,\mathrm{d}\xi}. \tag{17}$$

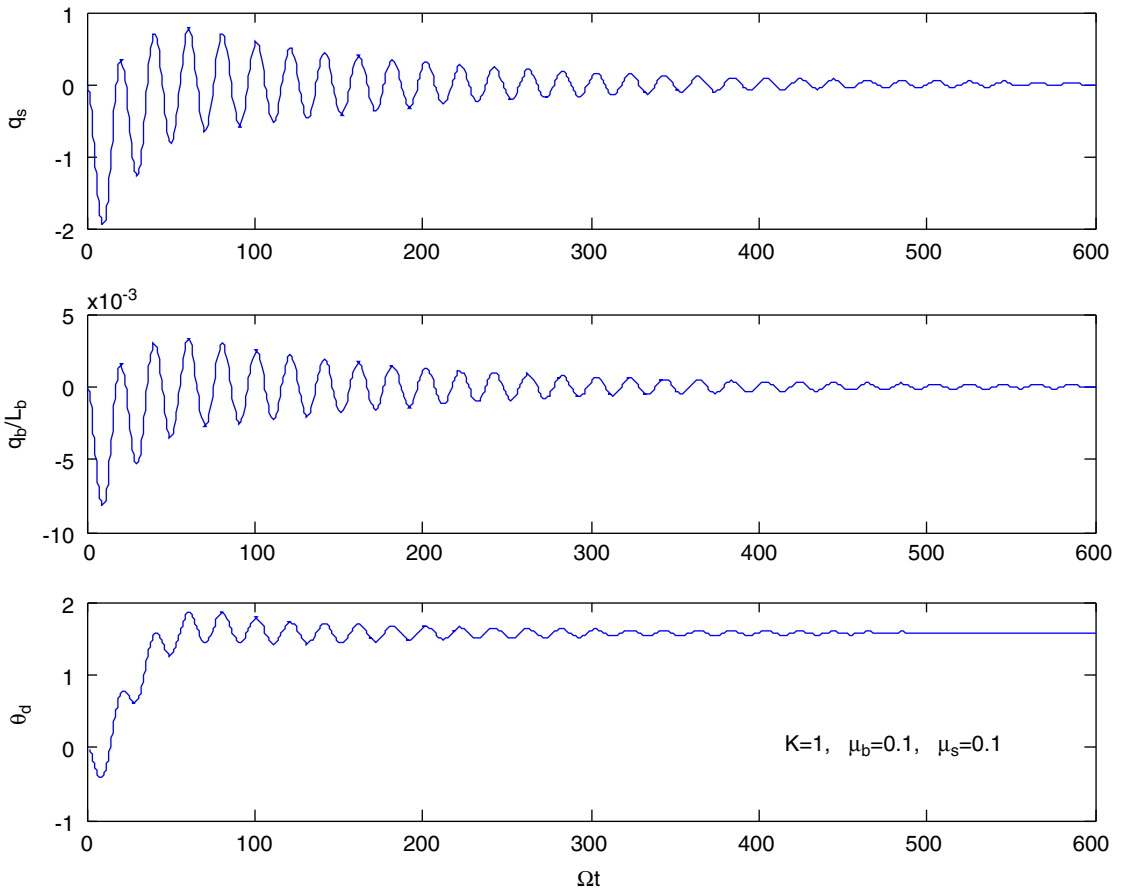

Fig. 6. Shaft, beam and disk response for $K = 1$, $\mu_b = 0.1$, $\mu_s = 0.1$.

Beam mode participation factor is

$$u_b = \frac{\int_0^1 ((r/l_b) + \xi)\phi_b(\xi)\,\mathrm{d}\xi}{\int_0^1 \phi_b^2(\xi)\,\mathrm{d}\xi}. \tag{18}$$

Here r/l_b is the disk radius to beam length ratio. In Eq. (10), beam generalized coordinate q_b is defined as q_b/l_b.

Beam mass moment of inertia with respect to the origin O is

$$J_{bo} = \int_0^{l_b} m_b(r + x)^2\,\mathrm{d}x. \tag{19}$$

Shaft polar mass moment of inertia is

$$J_s = \int_0^{l_s} \rho I_p\,\mathrm{d}z. \tag{20}$$

Total mass moment of inertia is

$$J_T = J_d + J_{bo} + J_s. \tag{21}$$

For the elastic shaft the following mode equation is obtained [12]:

$$\phi_s(z) = A\,\sin(\beta_s z), \quad 0 \leqslant z \leqslant l_s. \tag{22}$$

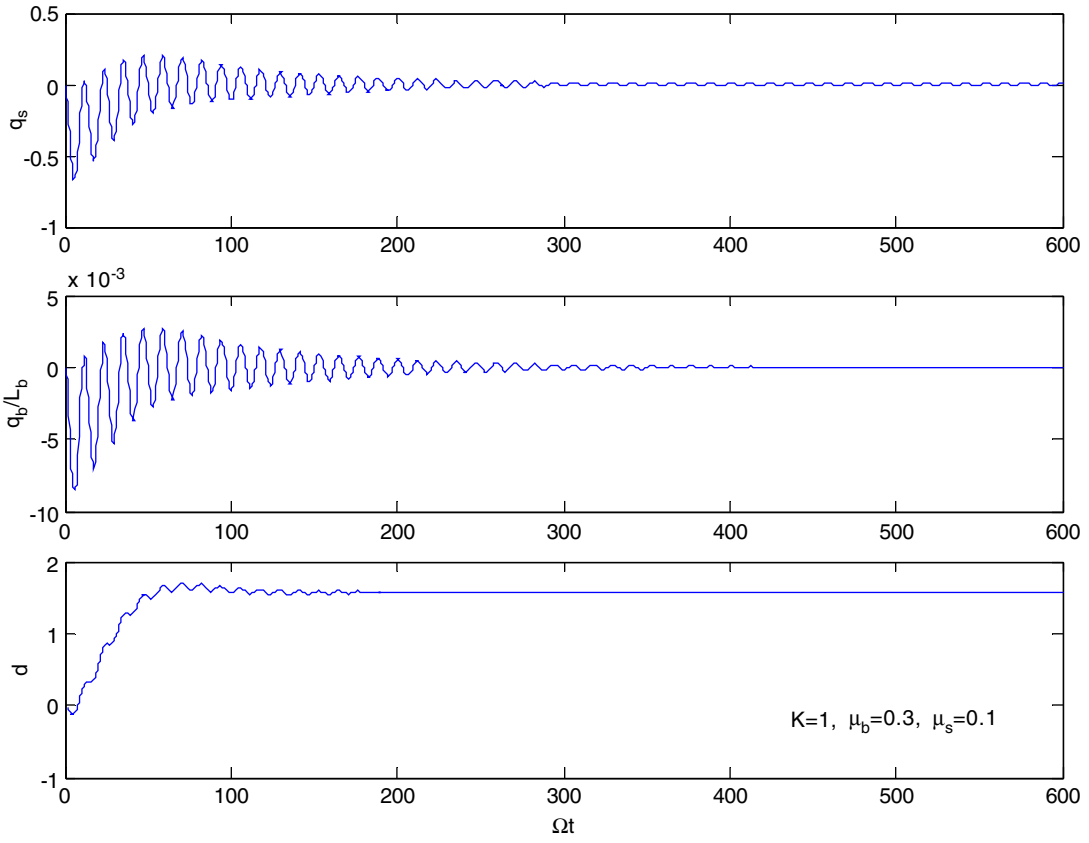

Fig. 7. Shaft, beam and disk response for $K = 1$, $\mu_b = 0.3$, $\mu_s = 0.1$.

Frequency equation of the shaft is obtained by using the following boundary condition:

$$GI_p \frac{\partial \psi}{\partial z}\bigg|_{z=l_s} = J_T \omega_s^2 \psi\big|_{z=l_s}. \tag{23}$$

The frequency equation is

$$\beta_s \tan \beta_s = \frac{J_s}{J_T} = \mu_s. \tag{24}$$

Here μ_s is the shaft inertia ratio. Shaft natural frequency is equal to

$$\omega_s = \beta_s \sqrt{\frac{G}{\rho l_s^2}}. \tag{25}$$

Eq. (24) is solved for some μ_s values. Table 1 gives β_s and $\phi_s(l_s)$ values for some μ_s values.

For the elastic beam, mode function is given as [12]

$$\phi_b(\xi) = A \cosh \beta_b l_b \xi + B \sinh \beta_b l_b \xi + C \cos \beta_b l_b \xi + D \sin \beta_b l_b \xi, \quad 0 \leqslant \xi \leqslant 1. \tag{26}$$

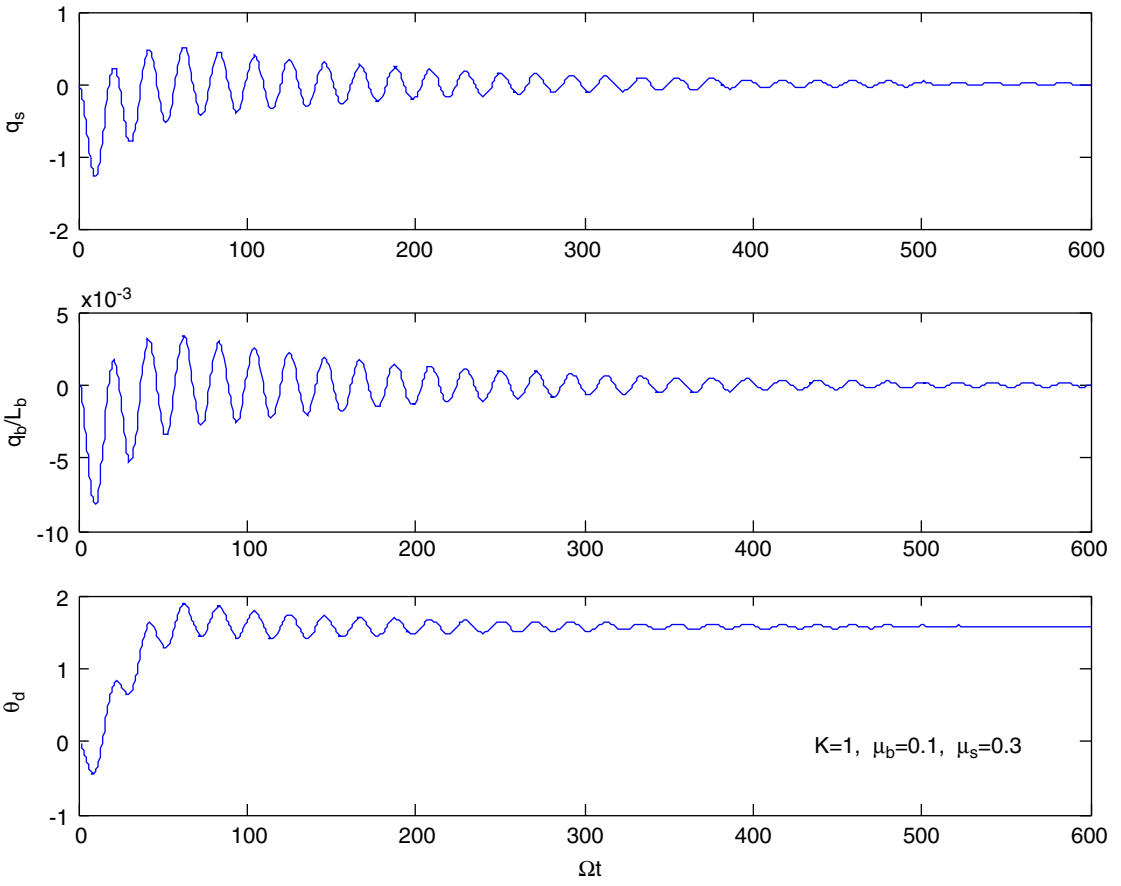

Fig. 8. Shaft, beam and disk response for $K = 1$, $\mu_b = 0.1$, $\mu_s = 0.3$.

Since the root of the flexible beam is not rigid because of the shaft flexibility, the following boundary conditions are assumed:

$$\begin{aligned} &y(0,t)=0,\\ &\mathrm{EI}y''(0,t)=\frac{\mathrm{GI}_p}{l_s}y'(0,t),\\ &y''(l_b,t)=0,\\ &y'''(l_b,t)=0. \end{aligned} \tag{27}$$

When these boundary conditions are used, frequency equation is obtained as

$$K(\beta_b l_b)(\sinh\beta_b l_b\cos\beta_b l_b-\cosh\beta_b l_b\sin\beta_b l_b)+\cosh\beta_b l_b\cos\beta_b l_b+1=0. \tag{28}$$

Here K is defined as the rigidity factor and given as

$$K=\frac{\mathrm{EI}/l_b}{\mathrm{GI}_p/l_s}=\frac{\text{Bending stiffness of beam per unit length}}{\text{Torsional stiffness of shaft per unit length}}. \tag{29}$$

Table 2 shows the values of $\beta_b l_b$ for different K values. If the torsional stiffness of the elastic shaft is infinite, K is equal to zero, which will correspond to a fixed-free beam boundary condition, if the torsional stiffness of the elastic shaft is zero; K is equal to infinite, which will correspond to a hinged-free beam boundary condition.

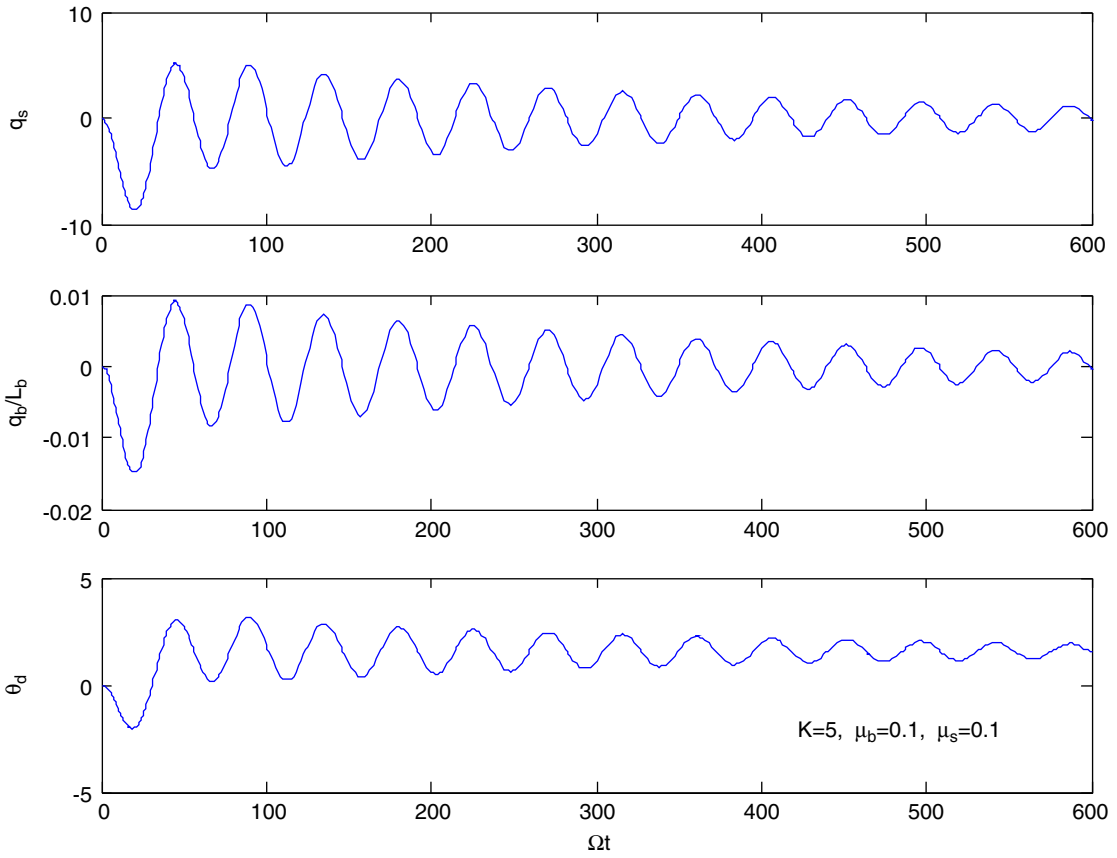

Fig. 9. Shaft, beam and disk response for $K=5$, $\mu_b=0.1$, $\mu_s=0.1$.

The beam natural frequency is equal to

$$\omega_{bi} = (\beta_b l_b)_i^2 \sqrt{\frac{\mathrm{EI}}{m_b l_b^4}}, \quad i = 1, 2, 3 \ldots. \tag{30}$$

To obtain nondimensional form of the equations, new time is defined as

$$\tau = \Omega t, \quad \Omega = \sqrt{\frac{\mathrm{EI}}{m_b l_b^4}}. \tag{31}$$

The following nondimensional equations are obtained:

$$\begin{aligned} &\ddot{q}_s + 2\zeta_s \beta_s \sqrt{\frac{\mu_{bs}}{K}} \dot{q}_s + \beta_s^2 \frac{\mu_{bs}}{K} q_s + \mu_b \gamma \ddot{q}_b = -\frac{1}{\phi_s(l_s)} \ddot{\theta}_m, \\ &\ddot{q}_b + 2\zeta_b (\beta_b l_b)^2 \dot{q}_b + (\beta_b l_b)^4 q_b + \phi_s(l_s) \alpha \ddot{q}_s = -\alpha \ddot{\theta}_m. \end{aligned} \tag{32}$$

Here derivations are with respect to τ, the beam inertia ratio is

$$\mu_b = \frac{m_b l_b^3}{J_T}. \tag{33}$$

Beam-to-shaft inertia ratio is

$$\mu_{bs} = \frac{\mu_b}{\mu_s} = \frac{m_b l_b^3}{J_s}. \tag{34}$$

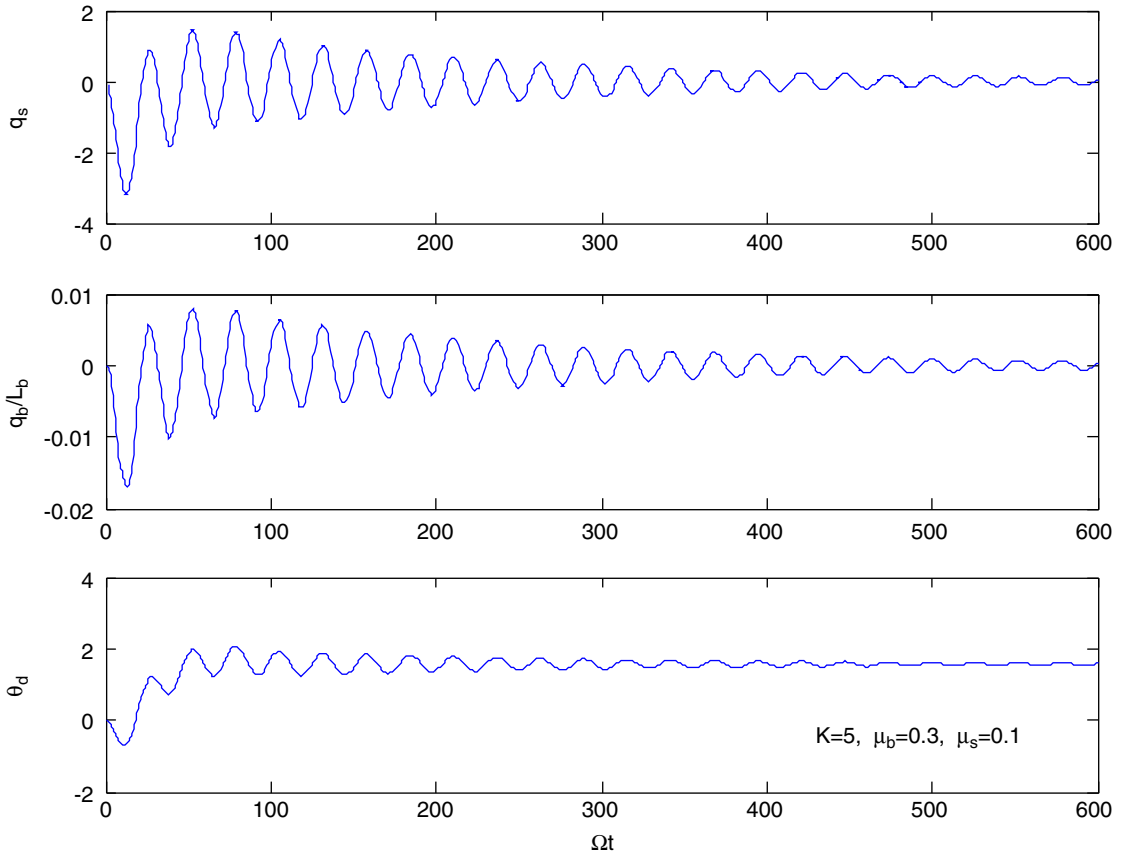

Fig. 10. Shaft, beam and disk response for $K = 5$, $\mu_b = 0.3$, $\mu_s = 0.1$.

α and γ are defined as

$$\alpha = \frac{\int_0^1 ((r/l_b) + \xi)\phi_b(\xi)\,\mathrm{d}\xi}{\int_0^1 \phi_b^2(\xi)\,\mathrm{d}\xi}, \tag{35}$$

$$\gamma = \frac{\int_0^1 ((r/l_b) + \xi)\phi_b(\xi)\,\mathrm{d}\xi}{\phi_s(l_s)}. \tag{36}$$

In these equations, the rigidity factor K, and the beam-to-shaft inertia ratio μ_{bs} and the beam inertia ratio μ_b are three independent variables. The shaft inertia ratio μ_s is already defined in Eq. (24) but three inertia ratios μ_b, μ_s and μ_{bs} are not independent from each other. If two of them are defined, the third will be calculated. In the simulations, μ_b and μ_s are used. The main objective of the work is to see the effect of the shaft and the beam flexibility on the behavior of the system. That is why, instead of introducing control system parameters into the equations, more general approach is used. It is assumed that the servomotor control system is producing a step input which can be produced by any second-order control system transfer function. Maximum rotational amplitude is $(\theta_m)_{\max}$. Input rotation function is given as

$$\theta_m = (\theta_m)_{\max}\left[1 - \frac{\mathrm{e}^{-\zeta_c(\omega_c/\Omega)\tau}}{\sqrt{1-\zeta_c^2}}\sin\left(\frac{\omega_c}{\Omega}\sqrt{1-\zeta_c^2}\tau + \phi\right)\right], \tag{37}$$

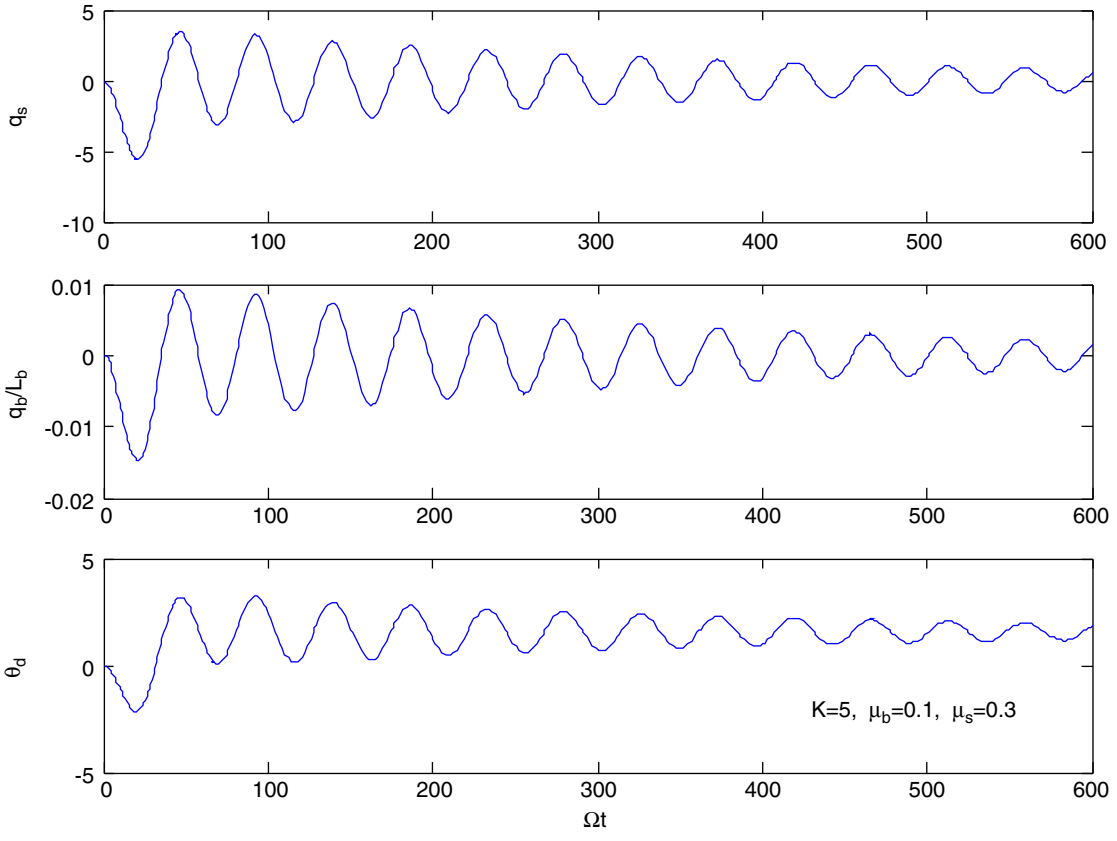

Fig. 11. Shaft, beam and disk response for $K = 5$, $\mu_b = 0.1$, $\mu_s = 0.3$.

the acceleration will be

$$\ddot{\theta}_m = (\theta_m)_{\max} \frac{1-2\zeta_c^2}{\sqrt{1-\zeta_c^2}} e^{-\zeta_c(\omega_c/\Omega)\tau} \sin\left(\frac{\omega_c}{\Omega}\sqrt{1-\zeta_c^2}\tau + \phi\right), \tag{38}$$

$$\phi = \tan^{-1}\frac{\sqrt{1-\zeta_c^2}}{\zeta_c}. \tag{39}$$

Here ζ_c is the control system damping ratio, ω_c/Ω is the nondimensional control system frequency.

3. Simulations

Equations given in Eq. (34) are solved for different values of K, μ_s and μ_b. Fig. 2 shows the rotation of the servomotor. Here $(\theta_m)_{\max}$ is assumed as $\pi/2$ rad, control system damping ratio ζ_c is assumed as 0.7 and the control system frequency ω_c/Ω is assumed as 0.06. For all calculations, disk radius to beam length ratio r/l_b is assumed as 0.2, viscous damping ratios ζ_s and ζ_b are assumed as 0.02. Figs. 3–5 show the elastic shaft vibration q_s, the beam vibration q_b/l_b and the disk rotation θ_d. In these calculations, the rigidity factor K is assumed as 0.1, which will give $(\beta_b l_b)_1 = 1.7227$. In this case, the shaft rigidity is very high and the system is close to a rigid shaft–elastic beam system. Figs. 3 and 4 show that if the beam inertia is increased relative to the shaft inertia,

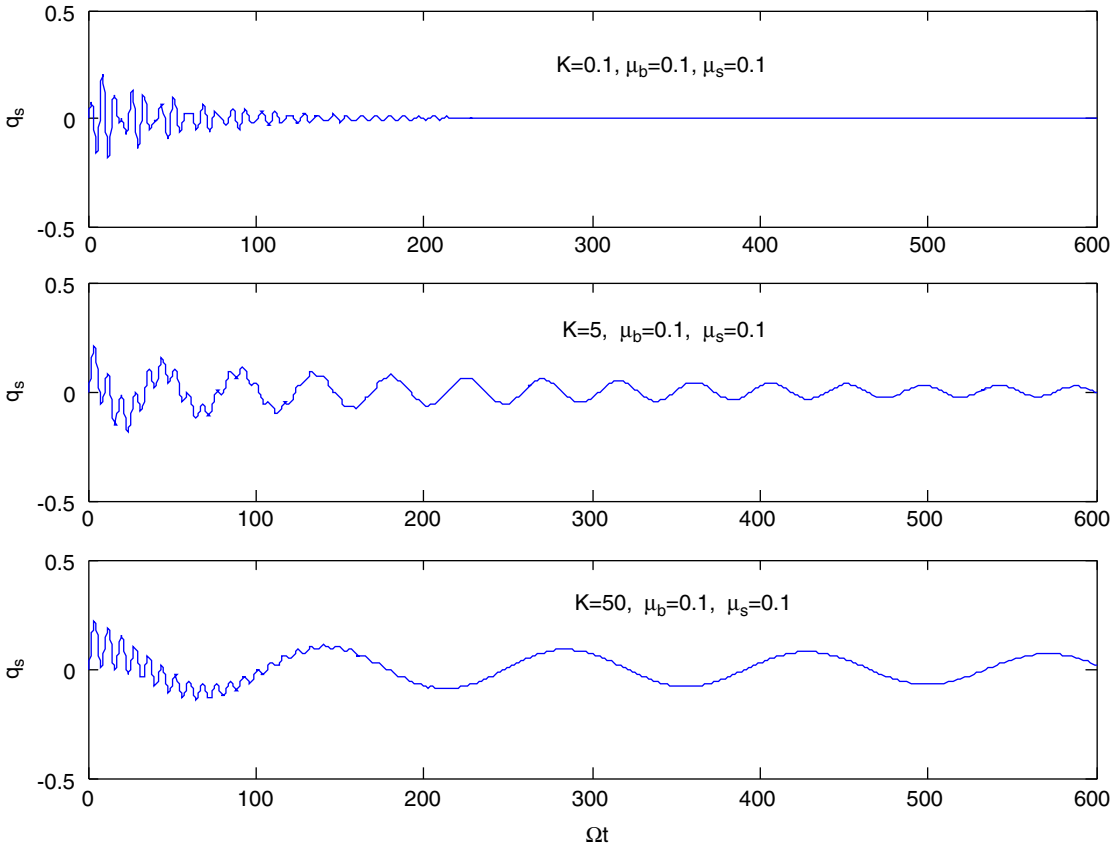

Fig. 12. Free vibration response for $K = 5$, $\mu_b = 0.1$, $\mu_s = 0.1$.

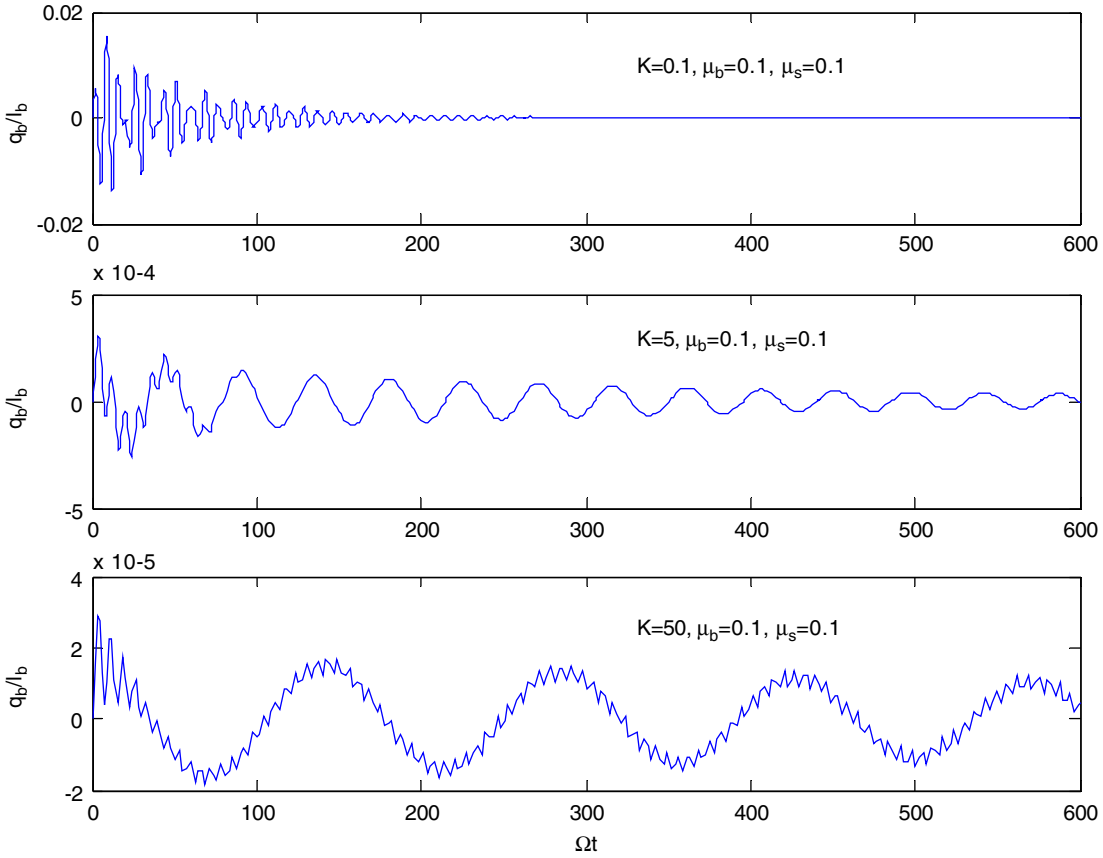

Fig. 13. Free vibration response for $K = 5$, $\mu_b = 0.1$, $\mu_s = 0.1$.

the system vibration frequency is increased and the shaft vibration amplitudes are decreased. Figs. 3 and 5 show that if the shaft inertia is increased relative to the beam inertia, system vibration frequency does not change but again shaft vibration amplitudes are decreased. In all cases, disk rotation is not affected much by the elasticity of the system. Figs. 6–8 show the case when the rigidity factor K is 1. In this case, shaft flexibility is 10 times bigger than the previous one. Figs. 6 and 7 show that when the beam inertia is increased relative to the shaft inertia, system vibration frequency in increased, shaft vibration amplitudes are decreased and also the effect of system elasticity on the disk rotation is reduced. Figs. 6 and 8 show that relative increase of the shaft inertia with respect to the beam inertia reduces the shaft vibration amplitudes but the beam vibration amplitudes remain the same. Figs. 9–11 show the case where the rigidity factor K is 5. Since the shaft flexibility is increased, all vibration amplitudes are proportionally increased. Settling time for the vibration is also longer. Comparison of Figs. 3, 6 and 9 shows that shaft vibration amplitudes are 10 times bigger for $K = 1$, and 40 times bigger for $K = 5$ than the vibration amplitudes of the case for $K = 0.1$.

Figs. 12 and 13 show the free vibration amplitudes of the flexible system if, either the shaft or the beam is given an initial displacement, assuming that there is no input rotation. Fig. 12 shows the shaft vibrations for three different rigidity factors. The beam is given initial displacement of $q_b/l_b = 0.1$. If the shaft is relatively rigid, high frequency but quickly damped shaft vibration is excited. If the shaft is relatively flexible, low-frequency sustained vibration is excited but for all cases the amplitudes are almost same. Fig. 13 shows the beam vibrations if the shaft is given initial displacement of $q_s = 0.1$. If the shaft is relatively rigid, high frequency, quickly damped beam vibration is excited. If the shaft is relatively flexible, low-frequency sustained beam vibration is excited but high-frequency and very low amplitude vibration of the beam coexists. Beam vibration amplitudes get smaller while the shaft flexibility is increased.

4. Conclusion

In this study, elastic shaft–elastic beam system is modeled. The model consists of a servomotor, an elastic shaft, a disk and an elastic beam, which is attached to the disk. Equations are derived with respect to the generalized coordinates of the elastic beam and the elastic shaft by using the Lagrange method. Mode summation technique is assumed for the solution. Frequency equations and mode shapes for the beam and the shaft are obtained assuming that they are coupled. Governing equations for the general coordinates are obtained and nondimensionalized. Three independent parameters are defined: the rigidity factor, the beam inertia ratio, and the shaft inertia ratio with respect to the total inertia of the system. As an input, second-order control system step response is assumed. Effects of the defined parameters on the behavior of the coupled elastic shaft–elastic beam system are shown.

References

[1] A. El-Sinawi, M.N. Hamdan, Optimal vibration estimation of a nonlinear flexible beam mounted on a rotating compliant hub, *Journal of Sound and Vibration* 259 (4) (2003) 857–872.
[2] Y.M. Al-Nassar, B.O. Al-Bedoor, On the vibration of a rotating blade on a torsionally flexible shaft, *Journal of Sound and Vibration* 259 (5) (2003) 1237–1242.
[3] B.O. Al-Bedoor, A. Al-Sinawi, M.N. Hamdan, Nonlinear dynamic model of an inextensible rotating flexible arm supported on a flexible base, *Journal of Sound and Vibration* 251 (2002) 767–781.
[4] H. Diken, Precise trajectory tracking control of elastic joint manipulator, *AIAA Journal of Guidance* 19 (3) (1996) 715–718.
[5] H. Diken, Frequency response characteristics of a single-link flexible joint manipulator and possible trajectory tracking, *Journal of Sound and Vibration* 233 (2) (2000) 179–194.
[6] H. Diken, Effect of shaft flexibility on control system parameters, *ASME Journal of Vibration and Acoustics* 122 (2000) 222–226.
[7] A. Ankarali, H. Diken, Vibration control of an elastic manipulator link, *Journal of Sound and Vibration* 204 (1) (1997) 162–170.
[8] H. Diken, Vibration control of a rotating Euler–Bernoulli beam, *Journal of Sound and Vibration* 232 (3) (2000) 541–551.
[9] O. Kopmaz, K.S. Anderson, On the eigen-frequencies of a flexible arm driven by a flexible shaft, *Journal of sound and vibration* 240 (2001) 679–704.
[10] F. Xi, R.G. Fenton, Coupling effect of flexible link and flexible joint, *International Journal of Robotics Research* 13 (1994) 443–453.
[11] F. Xi, R.G. Fenton, B. Tabarrok, Coupling effects in a manipulator with both a flexible link and joint, *Journal of Dynamic Systems, Measurement, and Control* 116 (1994) 826–831.
[12] W.T. Thomson, *Theory of Vibration with Applications*, second ed., Prentice-Hall, Englewood Cliffs, NJ, 1981.